Article

# Affinity of Amphiphilic Molecules to Air/Water Surface

Chi Minh Phan*

Read Online

ACCESS | Metrics & More | Article Recommendations

ABSTRACT: The affinity of amphiphiles to the water/air surface was modeled by adapting Eberhart's equation. The proposed method successfully describes surface tension for all amphiphilic structures, including alkanols, carboxylic acids, nonionic, ionic, and Gemini surfactants. The model is more effective than conventional analysis for amphiphiles with multiple ionic states. The prediction was consistently validated at different temperatures and non-aqueous solvents. The modeling results show a linear correlation between surface affinity and hydrophobicity/hydrophilicity. For alkanols, the affinity increment is 2.84 kJ/mol per CH_2 group, the same as the reported hydrophobic energy from monomer to aggregate for nonionic surfactants. For carboxylic acids, the affinity increment per CH_2 group is 3.18 kJ/mol, incorporating the degree of acid dissociation. The affinity−hydrophilicity correlation is approximately −0.22 kJ/mol per oxyethylene group. The affinity constant can be obtained for all classes of amphiphiles to clarify the relationship between the molecular structure and surface activity.
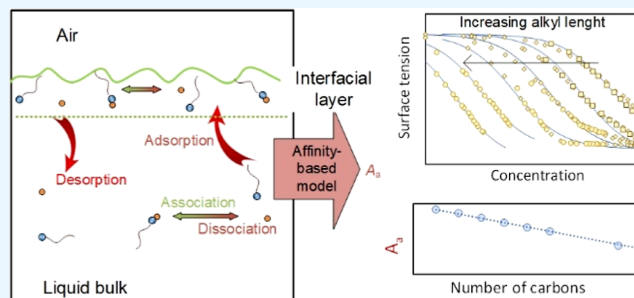
1. INTRODUCTION

The interfacial layer of aqueous solutions plays a central role in many processes, including evaporation,[1] cloud aerosol stability,[2] dewetting/wetting,[3] and mass transfer on surface flow.[4] The classical treatment of surface tension by the Young−Laplace-Gauss equation considers the interface between solution and air as a capillary surface,[5] with a zero thickness. Recent advances, including molecular simulations, have provided new insights into the molecular arrangement within the interfacial layer, with a thickness of ∼1 nm.[6] However, the gap between nanoscaled simulation and macroscopic data remains substantial.[7]

In the literature, the surface tension data are often modeled by the Gibbs adsorption equation. The most common approach is integrating the Gibbs adsorption with Langmuir isotherm to provide the Szyszkowski equation[8]

$$\gamma(C_b) = \gamma_w - nRT\Gamma_m \ln\left[\frac{C_b}{A} + 1\right] \qquad (1)$$

where γ and γ_w are the surface tension at concentration C_b and water surface tension, respectively, and R and T are gas constant and absolute temperature. The two fitting parameters are Γ_m and A, defined by Langmuir's adsorption equation. The value of n is assumed independent of concentration and depends on the ionic state of the surfactant ($n = 1$ for nonionic surfactants, $n = 2$ for ionic surfactants).

Industrial surfactants, including detergents, are characterized by a long alkyl group with very low solubility (less than 0.01% by mole). The above equation has been applied to hundreds of industrial surfactants, as reviewed by Rosen.[8] In addition to

fitting the surface tension data to eq 1,[9] the surface adsorption can be experimentally obtained from neutron reflectometry. Recently, Penfold and co-workers re-examined the method by combining tension data with neutron reflectometry for three types of deuterated surfactants. They found that the application of the Gibbs equation is valid for nonionic surfactants,[10] while being limited to a specific range for anionic[11] and cationic[12] surfactants. However, they showed that the approach could not be applied to surfactants that undergo ion association such as carboxylic acids and Gemini surfactants.

In addition to the industrial amphiphiles, there is another group of much weaker amphiphiles, which are fully soluble in water, such as ethanol and 1-propanol. The application of Gibb adsorption isotherm to these molecules requires a quantification of the activity coefficient.[13,14] For these fully miscible amphiphiles, many alternative models have been proposed in the literature.[15−17] While these models can be applied to specific aqueous mixtures, a systematic description remains unclear. Between the strong surfactants and fully miscible short-chain organics, there is another group of amphiphiles with intermediate strength: the medium-chain carboxylic acids. This group is characterized by partial dissociation and partial
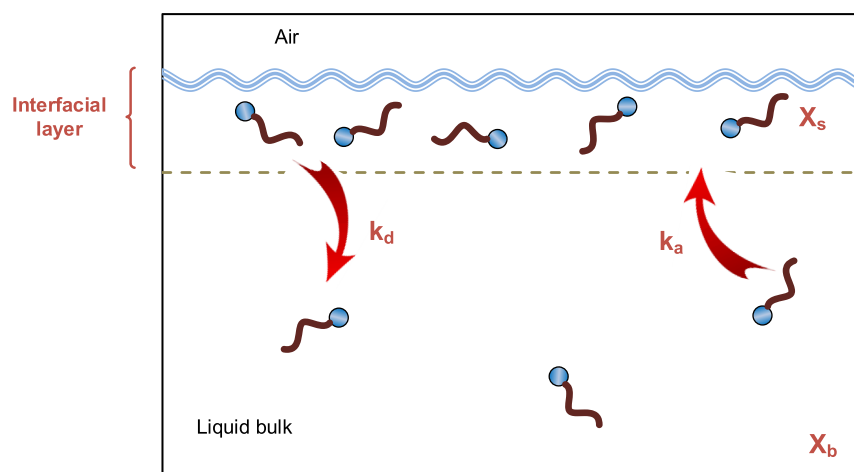
Figure 1. Equilibrium between the interfacial and bulk. Solvent molecules are omitted for clarity.

solubility (from 0.01 to 0.1% by mole).[18] These molecules are found naturally and play an important role in cloud aerosols and climate science.[19] The modeling of carboxylic acids, especially with partial dissociation near the surface, is mathematically complicated.[20]

In summary, all current modeling approaches are limited to a specific group of amphiphiles. The theoretical connection between the weak and completely soluble (e.g., methanol) and strong and partially soluble (e.g., alkyl trimethylammonium halide) amphiphile is unavailable. This study presents a new modeling approach, based on the thermodynamic equilibrium, to predict the surface tension and interfacial layer. The model aims to universally correlate the molecular structure and surface activity.

2. THEORY

In this model, the interfacial layer is considered a separate phase, limited by bulk liquid and air phases (Figure 1). The amphiphilic molecules have two processes: adsorption and desorption. The rates of the processes are

$$\text{rate of adsorption} = k_a X_b \tag{2}$$

$$\text{rate of desorption} = k_d X_s \tag{3}$$

where X_b and X_s are molar fractions within the interfacial layer and the bulk.

The equilibrium constant, K_a, is obtained by

$$K_a = \frac{k_a}{k_d} = \frac{X_s}{X_b} \tag{4}$$

Thermodynamics requires that chemical potential is the same between the two phases

$$\mu = \mu_b^0 + kT\log(X_b) = \mu_s^0 + kT\log(X_s) \tag{5}$$

where μ_b^0 and μ_s^0 are the standard part of the chemical potential in the bulk and interfacial layer.

The above framework has been validated for equilibrium between bulk monomers and aggregates (micelles, invert micelles, bilayer membrane, and vesicles) of soluble surfactants.[21] In this case, the interfacial layer in Figure 1 can be considered to be a monolayer with infinite area. Combining the above equations leads to

$$K_a = \frac{X_s}{X_b} = \exp\frac{\mu_b^0 - \mu_s^0}{kT} \tag{6}$$

The surface tension of the aqueous solution is the sum of the two-component surface tensions and is given by

$$\gamma(X_b) = \gamma_a X_s + \gamma_w[1 - X_s] \tag{7}$$

where $\gamma(X_b)$, γ_a, and γ_w are the surface tension of the mixture, pure organic compound, and pure water, respectively.

Recent molecular simulation[22] and neutron reflectometry[23] with water/ethanol have validated eq 7. The key challenge is the linkage between the interfacial and bulk compositions via a thermodynamic equation. The following equations are developed to address that gap.

The model requires the equilibrium constant of water, K_w (K_w is defined in the same form as in eq 4). Subsequently, a binary ratio between the two components is defined[24]

$$S = \frac{K_w}{K_a} = \exp\frac{(\mu_{b,w}^0 - \mu_{s,w}^0) - (\mu_{b,a}^0 - \mu_{s,a}^0)}{kT} \tag{8}$$

With this constant, the surface molar fraction is related to the bulk molar fraction

$$X_s = \frac{X_b}{X_b + S(1 - X_b)} \tag{9}$$

Consequently, eq 7 becomes

$$\gamma(X_b) = \frac{\gamma_a X_b + \gamma_w S(1 - X_b)}{X_b + S(1 - X_b)} \tag{10}$$

Equation 10, also known as Eberhart's equation,[a] has been successfully applied to water/ethanol[16] and many miscible systems, including aqueous and organic solvents.[25] The model implies that S is independent of X_b. For fully miscible liquids, the value of γ_a is experimentally obtainable. Consequently, eq 10 has only one fitting parameter, S. The pure solute surface tension condition is limited to small organic compounds.

For the molecules with limited solubility or that exist in solid form, the value of γ_a is physically unobtainable.[26] A new modeling approach allows a hypothetical value, γ_a^*. As a result, the equation has two fitting parameters. The physical interpretation and values of γ_a^* are discussed later.
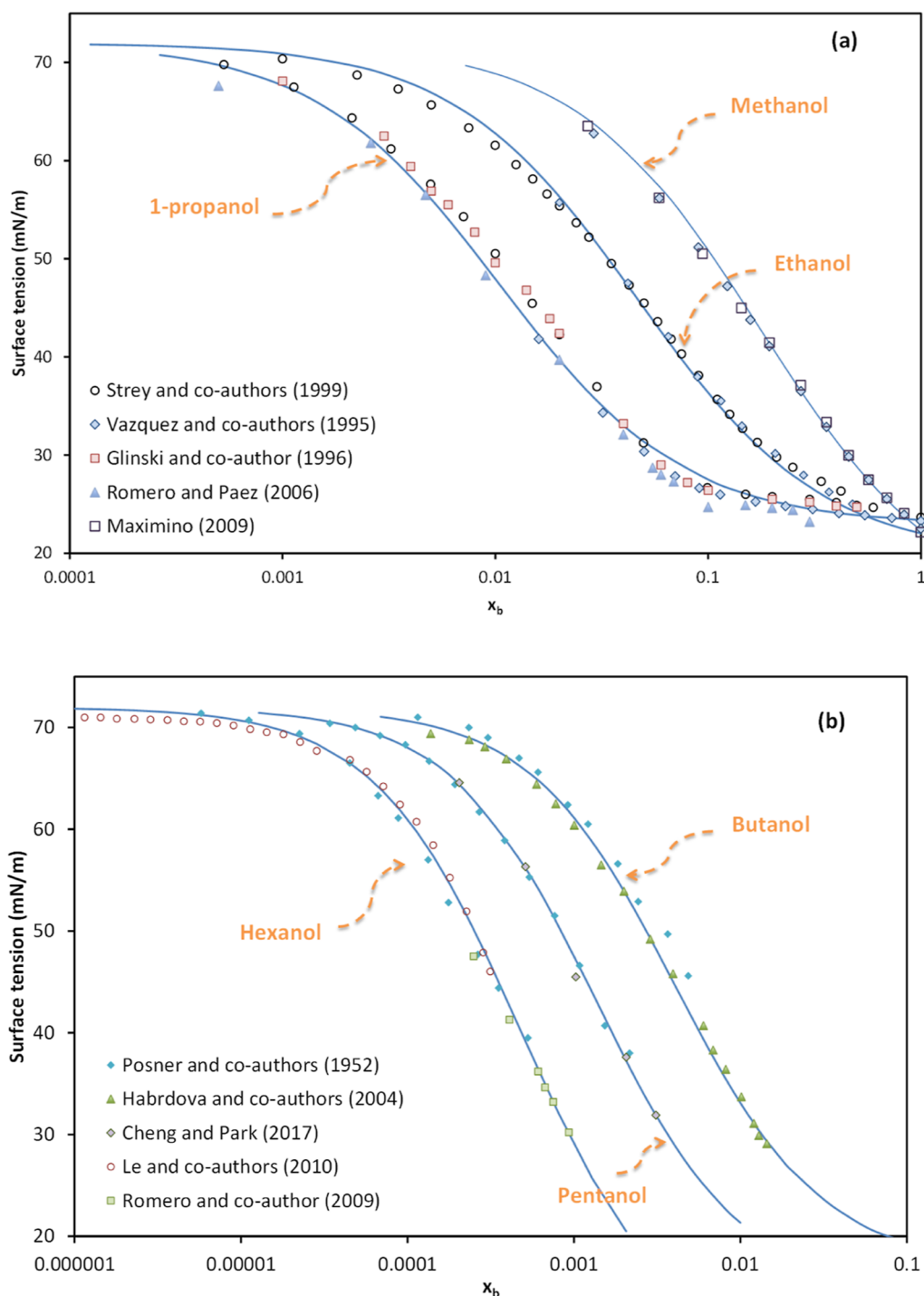
Figure 2. Modeling surface tension of *n*-alkanols (a) fully miscible[13,27−31] and (b) partially miscible[30,32−35] to solubility. All curves were generated by eq 10. Adapted from ref 46. Copyright (2019), Elsevier.

3. RESULTS AND DISCUSSION

First, eq 10 is applied, by least-squares fitting in Excel Solver, to six *n*-alkanols (Figure 2) and six carboxylic acids (Figure 3). The obtained best-fit values are tabulated in Table 1. The equation fits all data consistently. The fitting of fully miscible molecules (Figures 2a and 3a) has been discussed in the literature[15,16] and is presented for completeness. As the alkyl-chain length increases, the data shift to a surfactant-liked curve showing a gradual reduction in solubility (Figures 2b and 3b).

Subsequently, the model is applied to the surface tension[39] of three nonionic surfactants (Figure 4). This group of surfactants contains multiple groups of oxyethylene ($-C_2H_4O-$), which controls the "hydrophilicity" and "hydrophilic−lipophilic balance". The Triton X and other polyoxyethylenated series (Tween and Brij) are extensively used in many industries.[8] The values of the two fitting parameters are presented in Table 2. It should be noted that the model can predict the surface tension to the critical aggregate concentration (CAC) as with the conventional model.[40] A thermodynamic equilibrium can
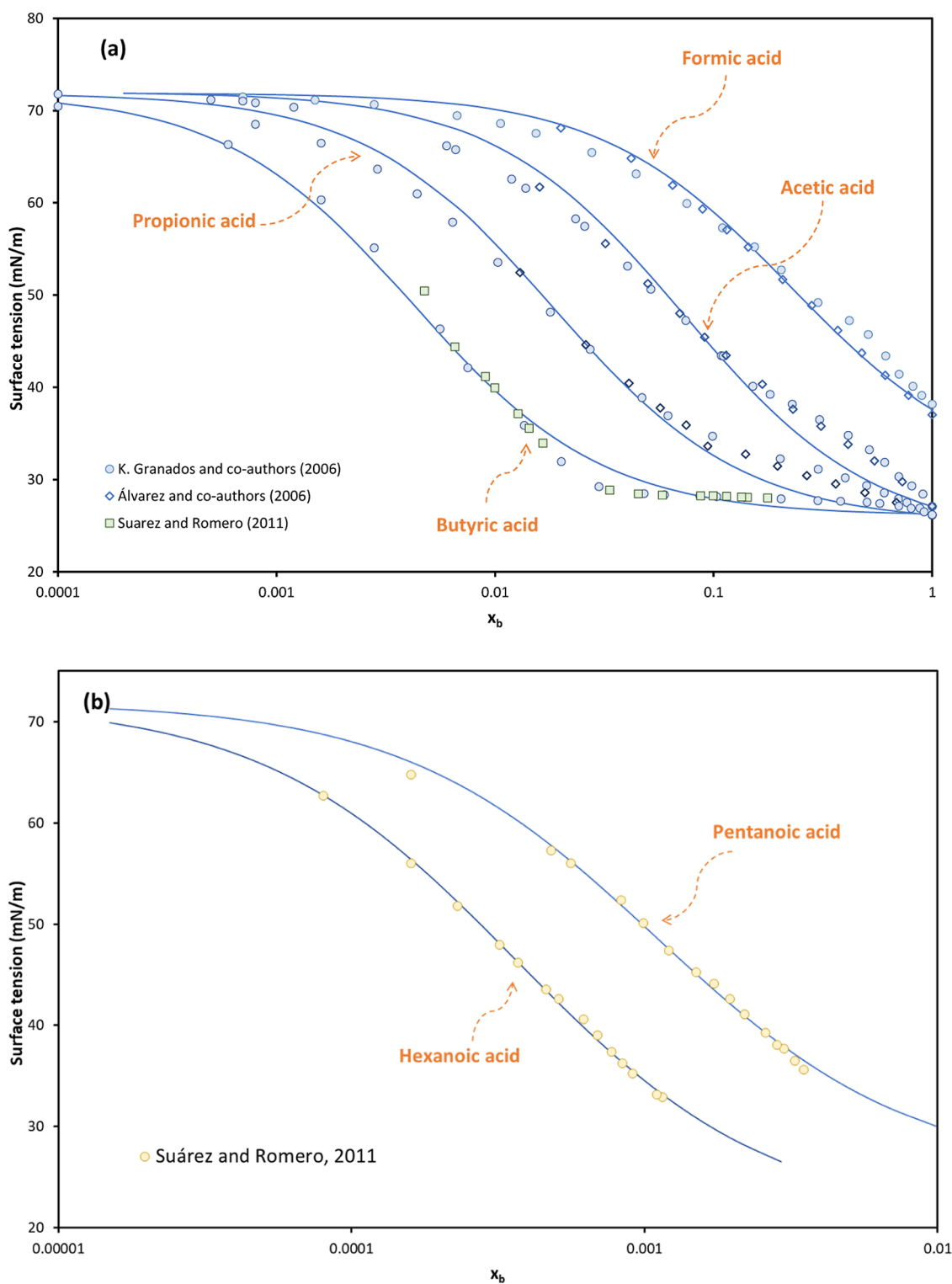
Figure 3. Modeling surface tension of carboxylic acids (a) fully miscible[36−38] and (b) partially miscible.[36] All curves were generated by eq 10.

explain the transition at the CAC, as discussed with micellar formation later.

Figures 3 and 4 show that eq 10 can predict the surface tension of partially soluble amphiphiles with an accuracy similar to that of the conventional model. Yet, the critical advantage of the equation over the conventional model is its applicability to other conditions. The main extensions are (1) changing temperature, (2) nonaqueous solvents, (3) the structure-surface affinity relationship, and (4) the degree of surfactant dissociation and

surfactants with multiple-charged groups. These implications are discussed in the following sections.

Before proceeding, the new term, specific surface affinity, is defined for each molecule

$$A_a = \mu_b^0 - \mu_s^0 \tag{11}$$

The affinity has a unit of kJ/mol,[b] similar to the Gibbs free energy of adsorption[25] or phase transferring energy[21] and

Table 1. Best-Fitted Adsorption for *n*-Alkanols and Carboxylic Acids (*: Fitted Values)

number of carbons	*n*-alkanol		carboxylic acid	
	S	γ_a (mN/m)	S	γ_a (mN/m)
1	0.150	22.33	0.184	37.60
2	0.0447	22.02	0.0679	27.10
3	0.0103	23.39	0.0181	26.17
4	0.00401	17.63*	0.00419	26.20
5	0.00135	14.57*	0.00110	25.40*
6	0.000476	8.62*	0.000366	20.89*

Table 2. Best-Fitted Adsorption for the Triton-X Surfactants

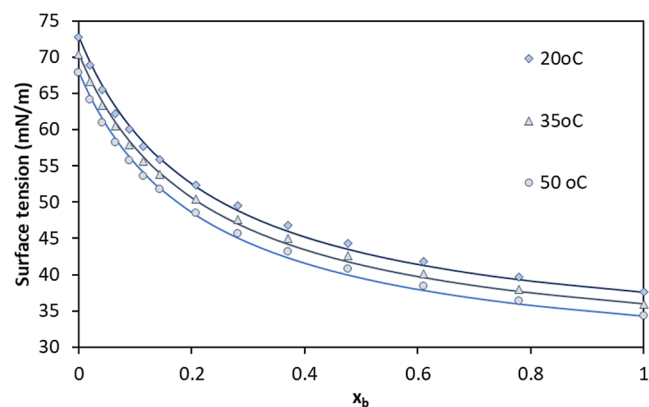| surfactant	average number of C_2H_4O group	$S \times 10^6$	γ_a (mN/m)
Triton X-100	9.5	0.180	24.92
Triton X-405	35	5.159	25.68
Triton X-705	55	8.526	23.37

Figure 5. Surface tension of the formic acid solutions at different temperatures (data are obtained from ref 37). All prediction curves are generated from the obtained S at 25 °C. Adapted with permission from ref 37. Copyright (1997), American Chemical Society.

quantitatively represents the tendency of the specific molecule to be exposed to the air. With the new quantity, eq 8 can be rearranged

$$kT \ln(S) = A_w - A_a \tag{12}$$

where A_w is the specific surface affinity of water.

3.1. Influence of Temperature. With increasing temperature, both the μ_b^0 and μ_s^0 increase. Being the difference between the two potentials, the affinity (A_a in eq 11) is less dependent on the temperature. Furthermore, both A_w and A_a should change in the same direction with increasing temperature. Consequently, it can be assumed that the net impact of changing temperature on the right-hand side of eq 12 is negligible. The value of S at any temperature can be linked to S at 25 °C by

$$\ln(S(T)) = \frac{298.15}{T+273.15} \ln(S(25°C)) \tag{13}$$

An example of the extension can be found in Figure 5. The predictions are obtained from S of formic acid/water at 25 °C (Table 1) without further fitting. The predictions are consistent with the experimental data at all temperatures. Applying the same predictions to other data provides a similar consistency.[37] Predicting the interfacial composition at elevated temperatures is essential to calculate the evaporation rate of the binary droplet.[41,42]

3.2. Nonaqueous Solvents. Since $\ln(S)$ is a difference between two affinities, a complementary rule can be applied to the three related binary mixtures.[24] To validate the rule, an intermediate molecule, ethylene glycol (EG), is considered. Ethylene glycol has a surface tension of 48 mN/m, almost the average value between that of water and ethanol. The surface tension of EG−water[34] and EG−ethanol[43] has already been reported.

The complementary rule from eq 12 gives

$$\ln(S_{ethanol-EG}) = \ln(S_{water-EG}) - \ln(S_{water-ethanol}) \tag{14}$$

where $S_{ethanol-EG}$, $S_{water-EG}$, and $S_{water-ethanol}$ are the coefficients of ethanol/EG, water/EG, and water/ethanol, respectively.

Since the value of $S_{water-ethanol}$ is already known, the data of EG−ethanol and EG−water can be fitted simultaneously, as
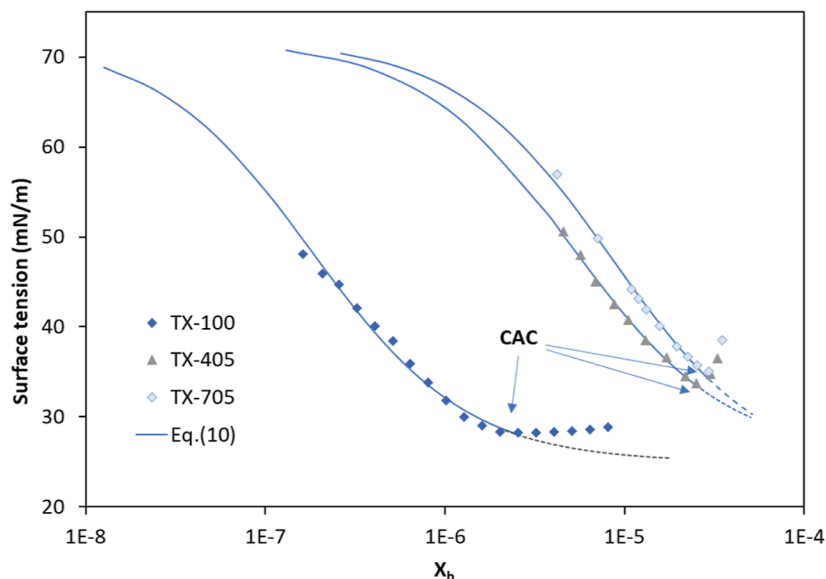

Figure 4. Modeling surface tension of nonionic surfactants (ref 39). The broken lines represent the extension of the model above CAC. Adapted from ref 39. Copyright (2018), John Wiley and Sons.
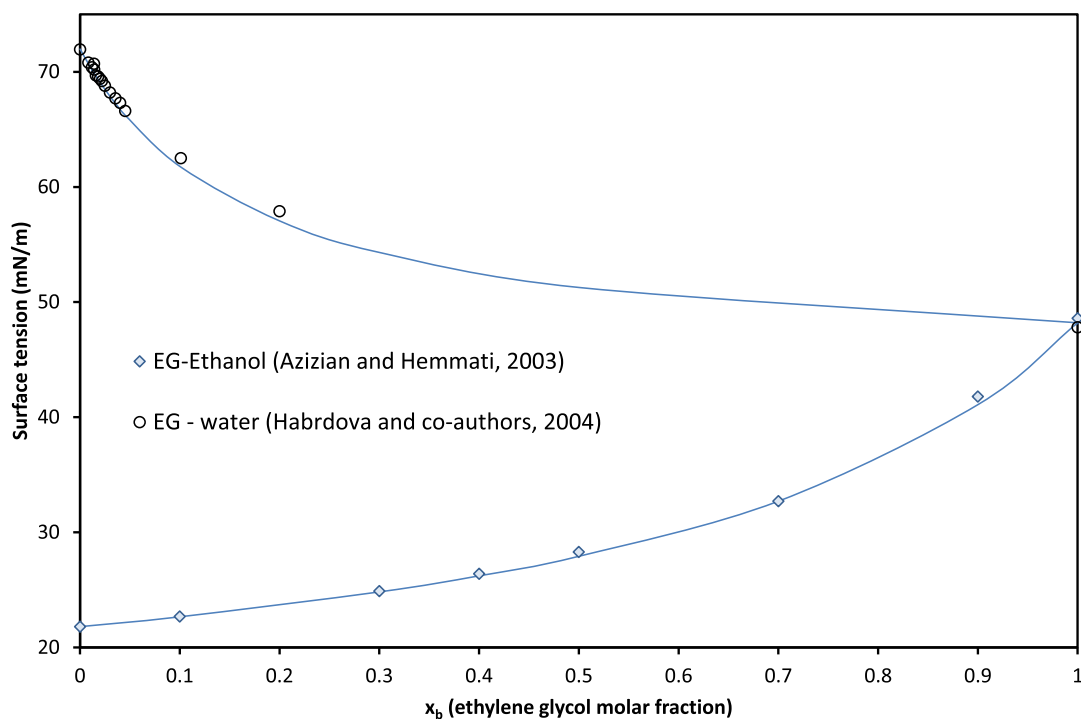
Figure 6. Simultaneous prediction of the surface tension of ethylene glycol mixtures with water and ethanol.
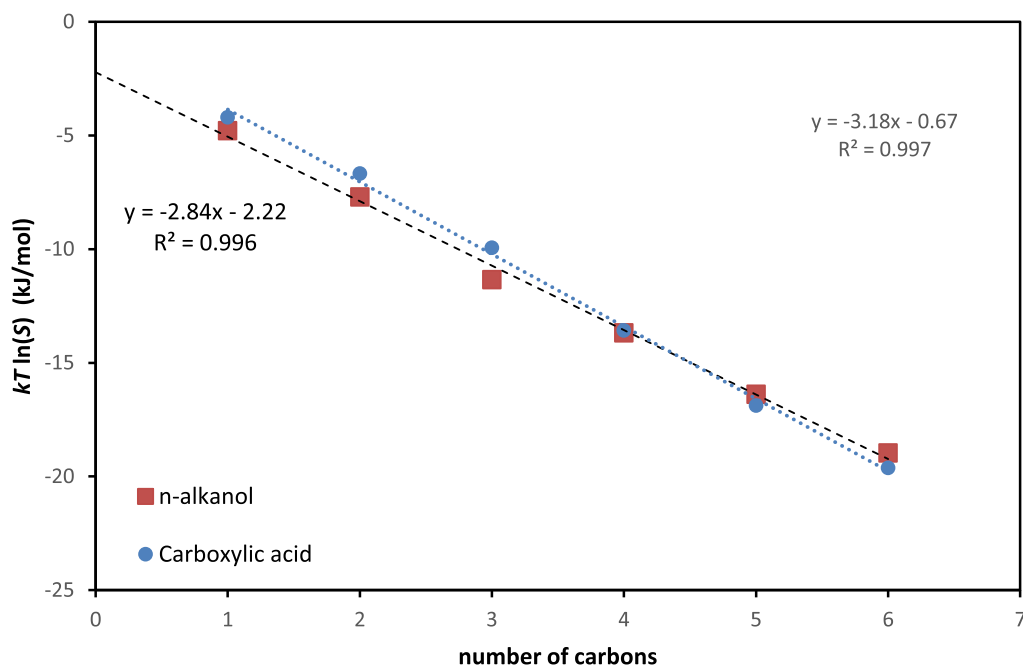

Figure 7. Relative affinity as a function of carbon length for *n*-alkanols and carboxylic acids (lines are linear regression).

shown in Figure 6. The best-fit value of $S_{water-EG}$ is 0.148. The data validate the rule in eq 14 and the consistency of the modeling approach.

3.3. Affinity-Hydrophobicity Correlation. From the data in Table 1, the relative affinity is plotted as a function of the carbon length (Figure 7). Both homologous series show clear linearity.

The slopes in Figure 7 represent the affinity increments per CH_2 group. For alkanols, this value is 2.84 kJ/mol per CH_2 group. The value is the same as Tahery's regression (which contains only three miscible alcohols).[25] In surfactant studies,

the hydrophobic energy increment, from the bulk to aggregate, has been summarized by Israelachvili (in Table 19.2 of ref 21).[21] For homologous straight-chain nonionic surfactants (alkyl polyoxyethylene monoethers), the reported increment was 2.9 kJ/mol per CH_2 group. The consistency between the two affinity increments validates the hydrophobic energy of the alkyl groups and the model.

The surface activity—alkyl relationship of surfactants has been central in surface science.[44] The author attempted to renew Langmuir's 1925 "principle of independent surface action"[45] via a multiple-component empirical model for alkanols.[46] While the

multiple-component model revealed a linearity similar to that in Figure 7, it was too complicated and incomplete. Equation 10 quantifies the alkyl hydrophobicity exceptionally well with a simple parameter.

The data can also be extrapolated to a lower limit of S. As the carbon length increases, S approaches zero, and the interfacial layer is more dominated by amphiphiles. It is well known that longer alkanoic acids, such as stearic acid, form a monolayer on an air/water surface (also known as Langmuir's monolayer). The layer is often considered insoluble and is widely used in surface studies.[21]

3.4. Partial Dissociation. Carboxylic compounds are weak acids with a low degree of dissociation. The increasing alkyl length reduces acidity and increases pK_a.[47] Thermodynamically, the degrees of acid dissociation differ between those of the bulk and the interfacial layer. For example, it has been shown that the surface-pK_a of medium-chain carboxylic acids is substantially higher than the bulk-pK_a.[48] A full adsorption modeling of all species (protonated/deprotonated acids and protons in both phases) would require a complicated mathematical model.[49,50]

As the data in Figure 3 were obtained without pH adjustment, eq 10 accounts for partial dissociation degrees in both the bulk and interfacial layers. The linearity of carboxylic data in Figure 7 indicates that the affinity incorporates partial dissociation very well. The increment for carboxylic acids is 3.18 kJ/mol per CH_2 group. The dissociation of acids and protons attributes the deviation from the alkanols value. For acids, the values of μ_s^0 and μ_b^0 represent the weighted average potential of the dissociated/associated species, which is also determined via thermodynamic equilibrium. The model can even provide a critical method to calculate the pK_a of short-chain acids, which are important for the cloud formation process and atmospheric chemistry.[51]

3.5. Affinity-Hydrophilicity Correlation. The affinity of nonionic surfactants in Table 2 is plotted in Figure 8.
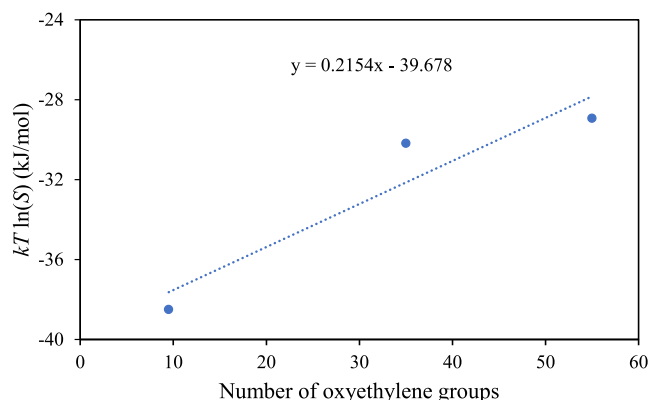

Figure 8. Affinity-hydrophilicity correlations for Triton-X surfactants.

It shows a negative correlation, with an energy of −0.22 kJ/mol per oxyethylene group. It should be noted that three Triton samples are industrial surfactants with mixtures of different numbers of oxyethylene. The reported numbers of oxyethylene in Table 2 are the average values. The impurities of the industrial products might lead to nonlinearity. Further study with precise control of the hydrophilic groups can clarify the increment energy.

3.6. Ionic Surfactants. The model can be easily applied to ionic surfactant solutions by converting the bulk concentration to the bulk molar fraction. Figure 9 shows examples of two
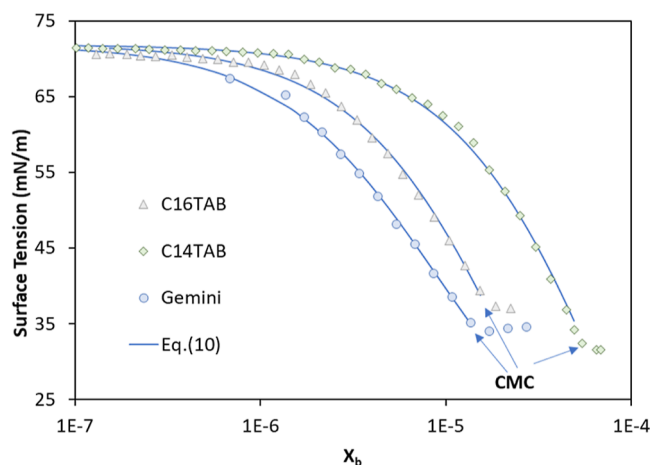

Figure 9. Modeling surface tension of C_nTAB (ref 53) and a Gemini surfactant (ref 54). Best-fitted parameters, C_{16}TAB: 2.54×10^{-5} and −16.3 mN/m, C_{14}TAB: 8.62×10^{-5} and −28.7 mN/m, Gemini: 9.04×10^{-6} and 10.4 mN/m. Adapted with permission from ref 53. Copyright (2013), American Chemical Society.

cationic surfactants,[52] cetyltrimethylammonium bromide (C_{16}TAB) and tetradecyltrimethylammonium bromide (C_{14}TAB), and a Gemini cationic surfactant ($C_{12}H_{25}N$-$(CH_3)_2$−$(CH_2)_3$−$N(CH_3)_2C_{12}H_{25}$ Br_2).[53]

The affinity increment of C_nTAB in Figure 9 is 1.51 kJ/mol per CH_2 group, which is smaller than the increment to the micelles (1.8 kJ/mol).[21] In this case, the affinity includes the full dissociation of − $(CH_3)_3N^+/Br^-$ pair and the hydration shell of Br^-, which is far stronger than a proton.[54] It should be noted that the two-parameter Szyszkowski equation, eq 1, produced a similar fitting quality with $n = 2$.[50] However, eq 1 assumes that C_nTA^+/Br^- is fully dissociated in the bulk and interfacial layers. The full dissociation is not supported by a recent study with combined NR/X-ray reflectometry on C_{16}TAB, which revealed that Br^- is closely condensed at the surface.[55] The condensation indicates a strong association of $C_{16}TA^+$ and Br^- within the interfacial layer. In this instance, the new model is more appropriate than the conventional approach.

The modeling of the Gemini surfactant is particularly effective. The Gemini surfactants form many diffident ionic states within the interfacial layer.[56] As discussed by Penfolds and co-workers, the Gibbs equation cannot be applied to Gemini surfactants.[11] Since thermodynamic rules also control the equilibria between these ionic states, eq 10 captures them all in a single parameter, as with the partial dissociation of carboxylic acids. The new model provides huge advantages over the conventional model, requiring many parameters for ionic states.[57,58]

The proposed modeling of ionic surfactant is more reliable than the conventional method[59] and overcomes the controversial saturated surface excess.[9] The obtained values of X_s can be combined with Gibbs's surface excess via the thickness of the interfacial layer.[23] Conversely, the interfacial molar composition might be more relevant to surface chemistry. For instance, the interfacial composition is easier to collaborate with molecular dynamics[6] or density gradient theory[60] simulations. The obtained X_s can provide critical information to neutron reflectometry[61] for predicting the thickness of the interfacial layer. The molar water composition, $1 − X_s$, can complement the vibrational sum-frequency generation[62] to understand the molecular orientation. The predicted composition can be

combined with surface potential data[63] to calculate the capacitance of the surfactant layer.

The thermodynamic equation can also explain the break in the surface tension data near the critical micelle concentration (CMC) or CAC, such as in Figures 4 and 9. At a high concentration, the surfactant molecules coexist in three states: the bulk, the interfacial layer, and micelles/aggregates.[64] The equilibrium in eq 4 is extended to

$$\mu = \mu_b^0 + kT\log(X_b) = \mu_s^0 + kT\log(X_s)$$
$$= \mu_m^0 + \frac{kT}{M}\log\left(\frac{X_m}{M}\right) \tag{15}$$

where μ_m^0, M, and X_m are the standard potential, aggregate number, and concentration of micelles/aggregates, respectively.

The thermodynamic equilibrium between X_b and X_m has led to the well-established calculation of the critical micelle concentration[21]

$$(X_b)_{\text{critical}} = \text{CMC} \approx \exp\left(\frac{\mu_m^0 - \mu_b^0}{kT}\right) \tag{16}$$

The same rule can apply to the surface molar fraction

$$(X_s)_{\text{critical}} \approx \exp\left(\frac{\mu_m^0 - \mu_s^0}{kT}\right) \tag{17}$$

Equation 17 indicates a maximum value of X_s, which is determined by the potentials of surface and micelle phases. The limit of X_s explains why a strong surfactant, such as C_{16}TAB, can only reduce the water surface tension to ~36 mN/m.[65] Conversely, butyric acid can reduce the water tension to 22 mN/m, despite being a "weak" surfactant.

3.7. Interpretation of γ_a for Surfactants. The value of γ_a for long molecules can be justified by considering the value of K_a. Mathematically, the value of γ_a corresponds to the composition of $X_s = 1$. The data in Table 1 show that S decreases, and K_a increases, with increasing alkyl length. The value corresponds to the replacement ratio between the surface and the bulk. The smaller S indicates that more water molecules are being replaced by a surfactant molecule. Consequently, γ_a decreases with an increasing alkyl-chain length (Table 1). For ionic surfactants, replacement is massively increased and, thus, γ_a becomes negative. For polyoxyethylene surfactants (Table 2), the relative water/surfactant ratio is large (oxyethylene can form H-bonds with water). As a result, the value of γ_a for nonionic surfactant is closer to the surface tension at CAC.

3.8. Affinity of Solvents. Two important observations can be made regarding the relative affinity (eq 12). First, the extension of alkanols regression (Figure 7) indicates that the water affinity is small but nonzero.[c] The small affinity (less than the affinity of all amphiphiles) is consistent with the notion of strong water−water bonds,[21] which generates higher boiling point and surface tension than other liquids. The nonzero value of affinity indicates that water also has a tendency to be exposed to air, as evidenced by the free −OH group.[66] Second, the water-based affinity can be transferred to another solvent via the complementary rule in eq 14. Indeed, the rule can predict the surface composition of two molecules with similar surface tension, such as methanol/propanol mixtures or a Triton surfactant in oil. As a result, the obtained relative affinity is as useful as the absolute affinity, A_a.

4. CONCLUSIONS

A new model applies to the surface tension data of all amphiphiles over many orders of concentration. The modeling framework is quantitatively validated for changing temperature, alkyl hydrophobicity, oxyethylene hydrophilicity, and non-aqueous solvents. The affinity of carboxylic acids can capture the dissociation effect and lay a foundation to model the surface affinity of ionic surfactants. The modeling approach is applicable to the oil/water interfacial tension as well.

■ AUTHOR INFORMATION

Corresponding Author

    Chi Minh Phan − *Discipline of Chemical Engineering, WASM:MECE, Curtin University, Perth, Western Australia 6845, Australia;* ● orcid.org/0000-0002-1565-8193; Email: c.phan@curtin.edu.au

Complete contact information is available at: https://pubs.acs.org/10.1021/acsomega.3c06512

■ ADDITIONAL NOTES

[a]Replacing S by $1/S$, eq 9 returns to Eberhart's original form (eq 5 in ref 24).
[b]Conventional surfactant studies often used a "free energy of adsorption", which has the same unit. However, it has different physical meanings and mathematic definitions, for instance, eq (2.32) in ref 8.
[c]This model allows solvent to have a nonzero affinity. The Gibbs equation assumes chemical potential is the same between the bulk and surface.

■ REFERENCES

(1) Pahlavan, A. A.; Yang, L.; Bain, C. D.; Stone, H. A. Evaporation of Binary-Mixture Liquid Droplets: The Formation of Picoliter Pancake-like Shapes. *Phys. Rev. Lett.* **2021**, *127* (2), 024501.

(2) Farmer, D. K.; Cappa, C. D.; Kreidenweis, S. M. Atmospheric Processes and Their Controlling Influence on Cloud Condensation Nuclei Activity. *Chem. Rev.* **2015**, *115* (10), 4199−4217.

(3) Ireland, P. M. Some Curious Observations of Soap Film Contact Lines. *Chem. Eng. Sci.* **2008**, *63* (8), 2174−2187.

(4) Doppelhammer, N.; Puttinger, S.; Pellens, N.; Voglhuber-Brunnmaier, T.; Asselman, K.; Jakoby, B.; Kirschhock, C. E. A.; Reichel, E. K. Generation and Observation of Long-Lasting and Self-Sustaining Marangoni Flow. *Langmuir* **2023**, *39* (22), 7804−7810.

(5) Finn, R. Capillary Surface Interactions. *Not. AMS* **1999**, *46*, 770−781.

(6) Tillotson, M. J.; Diamantonis, N. I.; Buda, C.; Bolton, L. W.; Müller, E. A. Molecular Modelling of the Thermophysical Properties of Fluids: Expectations, Limitations, Gaps and Opportunities. *Phys. Chem. Chem. Phys.* **2023**, *25* (18), 12607−12628.

(7) Peng, M.; Nguyen, A. V. Adsorption of Ionic Surfactants at the Air-Water Interface: The Gap between Theory and Experiment. *Adv. Colloid Interface Sci.* **2020**, *275*, 102052.

(8) Rosen, M. J.; Kunjappu, J. T. *Surfactants and Interfacial Phenomena*; Wiley, 2012.

(9) Menger, F. M.; Rizvi, S. A. A. Relationship between Surface Tension and Surface Coverage. *Langmuir* **2011**, *27* (23), 13975−13977.

(10) Li, P. X.; Li, Z. X.; Shen, H.-H.; Thomas, R. K.; Penfold, J.; Lu, J. R. Application of the Gibbs Equation to the Adsorption of Nonionic Surfactants and Polymers at the Air-Water Interface: Comparison with Surface Excesses Determined Directly Using Neutron Reflectivity. *Langmuir* **2013**, *29* (30), 9324−9334.

(11) Xu, H.; Li, P. X.; Ma, K.; Thomas, R. K.; Penfold, J.; Lu, J. R. Limitations in the Application of the Gibbs Equation to Anionic Surfactants at the Air/Water Surface: Sodium Dodecylsulfate and Sodium Dodecylmonooxyethylenesulfate Above and Below the CMC. *Langmuir* **2013**, *29* (30), 9335−9351.

(12) Li, P. X.; Thomas, R. K.; Penfold, J. Limitations in the Use of Surface Tension and the Gibbs Equation To Determine Surface Excesses of Cationic Surfactants. *Langmuir* **2014**, *30* (23), 6739−6747.

(13) Strey, R.; Viisanen, Y.; Aratono, M.; Kratohvil, J. P.; Yin, Q.; Friberg, S. E. On the Necessity of Using Activities in the Gibbs Equation. *J. Phys. Chem. B* **1999**, *103* (43), 9112−9116.

(14) Yano, Y. F. Correlation between Surface and Bulk Structures of Alcohol-Water Mixtures. *J. Colloid Interface Sci.* **2005**, *284* (1), 255−259.

(15) Tönsmann, M.; Ewald, D. T.; Scharfer, P.; Schabel, W. Surface Tension of Binary and Ternary Polymer Solutions: Experimental Data of Poly(Vinyl Acetate), Poly(Vinyl Alcohol) and Polyethylene Glycol Solutions and Mixing Rule Evaluation over the Entire Concentration Range. *Surface. Interfac.* **2021**, *26*, 101352.

(16) Santos, M. S. C. S.; Reis, J. C. R. A Semi-Empirical Equation for Describing the Surface Tension of Aqueous Organic Liquid Mixtures. *Fluid Phase Equilib.* **2016**, *423*, 172−180.

(17) Piñeiro, Á.; Brocos, P.; Amigo, A.; Gracia-Fadrique, J.; Guadalupe Lemus, M. Extended Langmuir Isotherm for Binary Liquid Mixtures. *Langmuir* **2001**, *17* (14), 4261−4266.

(18) Phan, C. M. *Ionization of Surfactants at the Air-Water Interface*; Elsevier Inc., 2018.

(19) Chebbi, A.; Carlier, P. Carboxylic Acids in the Troposphere, Occurrence, Sources, and Sinks: A Review. *Atmos. Environ.* **1996**, *30* (24), 4233−4249.

(20) Luo, M.; Wauer, N. A.; Angle, K. J.; Dommer, A. C.; Song, M.; Nowak, C. M.; Amaro, R. E.; Grassian, V. H. Insights into the Behavior of Nonanoic Acid and Its Conjugate Base at the Air/Water Interface through a Combined Experimental and Theoretical Approach. *Chem. Sci.* **2020**, *11* (39), 10647−10656.

(21) Israelachvili, J. N. *Intermolecular and Surface Forces*; 3rd ed.; Elsevier, 2011.

(22) Phan, C. M.; Nguyen, C. V.; Pham, T. T. T. Molecular Arrangement and Surface Tension of Alcohol Solutions. *J. Phys. Chem. B* **2016**, *120* (16), 3914−3919.

(23) Hyde, A. E.; Ohshio, M.; Nguyen, C. V.; Yusa, S.; Yamada, N. L.; Phan, C. M. Surface Properties of the Ethanol/Water Mixture: Thickness and Composition. *J. Mol. Liq.* **2019**, *290*, 111005.

(24) Eberhart, J. G. The Surface Tension of Binary Liquid Mixtures. *J. Phys. Chem.* **1966**, *70* (4), 1183−1186.

(25) Tahery, R.; Modarress, H.; Satherley, J. Surface Tension Prediction and Thermodynamic Analysis of the Surface for Binary Solutions. *Chem. Eng. Sci.* **2005**, *60* (17), 4935−4952.

(26) Wexler, A. S.; Dutcher, C. S. Statistical Mechanics of Multilayer Sorption: Surface Tension. *J. Phys. Chem. Lett.* **2013**, *4* (10), 1723−1726.

(27) Vazquez, G.; Alvarez, E.; Navaza, J. M. Surface Tension of Alcohol Water + Water from 20 to 50 .degree.C. *J. Chem. Eng. Data* **1995**, *40* (3), 611−614.

(28) Glinski, J.; Chavepeyer, G.; Platten, J. Surface Properties of Diluted Aqueous Solutions of Normal Propyl Alcohol. *J. Chem. Phys.* **1996**, *104* (21), 8816−8820.

(29) Belda Maximino, R. Surface Tension and Density of Binary Mixtures of Monoalcohols, Water and Acetonitrile: Equation of Correlation of the Surface Tension. *Phys. Chem. Liq.* **2009**, *47* (5), 475−486.

(30) Cheng, K. K.; Park, C. Surface Tension of Dilute Alcohol-Aqueous Binary Fluids: N-Butanol/Water, n-Pentanol/Water, and n-Hexanol/Water Solutions. *Heat Mass Tran.* **2017**, *53* (7), 2255−2263.

(31) Romero, C. M.; Paéz, M. S. Surface Tension of Aqueous Solutions of Alcohol and Polyols at 298.15 K. *Phys. Chem. Liq.* **2006**, *44* (1), 61−65.

(32) Le, T. N.; Phan, C. M.; Ang, H. M. Influence of Hydrophobic Tail on the Adsorption of Isomeric Alcohols at Air/Water Interface. *Asia-Pac. J. Chem. Eng.* **2012**, *7* (2), 250−255.

(33) Posner, A. M.; Anderson, J. R.; Alexander, A. E. The Surface Tension and Surface Potential of Aqueous Solutions of Normal Aliphatic Alcohols. *J. Colloid Sci.* **1952**, *7* (6), 623−644.

(34) Habrdová, K.; Hovorka, S. ·.; Bartovská, L. Concentration Dependence of Surface Tension for Very Dilute Aqueous Solutions of Organic Nonelectrolytes. *J. Chem. Eng. Data* **2004**, *49* (4), 1003−1007.

(35) Romero, C. M.; Jiménez, E.; Suárez, F. Effect of Temperature on the Behavior of Surface Properties of Alcohols in Aqueous Solution. *J. Chem. Thermodyn.* **2009**, *41* (4), 513−516.

(36) Suárez, F.; Romero, C. M. Apparent Molar Volume and Surface Tension of Dilute Aqueous Solutions of Carboxylic Acids. *J. Chem. Eng. Data* **2011**, *56* (5), 1778−1786.

(37) Álvarez, E.; Vázquez, G.; Sánchez-Vilas, M.; Sanjurjo, B.; Navaza, J. M. Surface Tension of Organic Acids + Water Binary Mixtures from 20 °C to 50 °C. *J. Chem. Eng. Data* **1997**, *42* (5), 957−960.

(38) Granados, K.; Gracia-Fadrique, J.; Amigo, A.; Bravo, R. Refractive Index, Surface Tension, and Density of Aqueous Mixtures of Carboxylic Acids at 298.15 K. *J. Chem. Eng. Data* **2006**, *51* (4), 1356−1360.

(39) Nguyen, T. B.; Phan, C. M. Influence of Temperature on the Surface Tension of Triton Surfactant Solutions. *J. Surfactants Deterg.* **2019**, *22* (2), 229−235.

(40) Fainerman, V. B.; Lylyk, S. V.; Aksenenko, E. V.; Makievski, A. V.; Petkov, J. T.; Yorke, J.; Miller, R. Adsorption Layer Characteristics of Triton Surfactants. *Colloids Surf. A Physicochem. Eng. Asp.* **2009**, *334* (1−3), 1−7.

(41) Nguyen, T. T. B.; Mitra, S.; Pareek, V.; Joshi, J. B.; Evans, G. M. Evaporation of a Sessile Binary Droplet on a Heated Spherical Particle. *Exp. Therm. Fluid Sci.* **2018**, *99*, 558−571.

(42) Shibata, Y.; Tanaka, K.; Asakuma, Y.; Nguyen, C. V.; Hoang, S. A.; Phan, C. M. Selective Evaporation of a Butanol/Water Droplet by Microwave Irradiation, a Step toward Economizing Biobutanol Production. *Biofuel Res. J.* **2020**, *7* (1), 1109−1114.

(43) Azizian, S.; Hemmati, M. Surface Tension of Binary Mixtures of Ethanol + Ethylene Glycol from 20 to 50 °C. *J. Chem. Eng. Data* **2003**, *48* (3), 662−663.

(44) Adamson, A. W.; Gast, A. P. *Physical Chemistry of Surfaces*, 6th ed.; Wiley, 1997.

(45) Langmuir, I. The Distribution and Orientation of Molecules. *Colloid Symposium Monograph*, 1925; pp 48−75.

(46) Phan, C. M. Independent Surface Action at the Air/Water Surface: A Renewed Concept via Artificial Neural Network. *Colloids Surf. A Physicochem. Eng. Asp.* **2019**, *567* (January), 319−324.

(47) Schürmann, G. Modelling pK_a of Carboxylic Acids and Chlorinated Phenols. *Mol. Inform.* **1996**, *15* (2), 121−132.

(48) Wellen, B. A.; Lach, E. A.; Allen, H. C. Surface pKa of Octanoic, Nonanoic, and Decanoic Fatty Acids at the Air-Water Interface: Applications to Atmospheric Aerosol Chemistry. *Phys. Chem. Chem. Phys.* **2017**, *19* (39), 26551−26558.

(49) Badban, S.; Hyde, A. E.; Phan, C. M. Hydrophilicity of Nonanoic Acid and Its Conjugate Base at the Air/Water Interface. *ACS Omega* **2017**, *2* (9), 5565−5573.

(50) Phan, C. M. Dissociation of Ionic Surfactants at the Air/Water Interface: Complete or Partial? *J. Phys. Chem. B* **2016**, *120* (31), 7681−7686.

(51) Gen, M.; Hibara, A.; Phung, P. N.; Miyazaki, Y.; Mochida, M. In Situ Surface Tension Measurement of Deliquesced Aerosol Particles. *J. Phys. Chem. A* **2023**, *127* (29), 6100−6108.

(52) Phan, C. M.; Le, T. N.; Nguyen, C. V.; Yusa, S. I. Modeling Adsorption of Cationic Surfactants at Air/Water Interface without Using the Gibbs Equation. *Langmuir* **2013**, *29* (15), 4743−4749.

(53) Nguyen, C. V.; Nguyen, T. V.; Phan, C. M. Dynamic Adsorption of a Gemini Surfactant at the Air/Water Interface. *Colloids Surf. A Physicochem. Eng. Asp.* **2015**, *482*, 365−370.

(54) Agmon, N.; Bakker, H. J.; Campen, R. K.; Henchman, R. H.; Pohl, P.; Roke, S.; Thämer, M.; Hassanali, A. Protons and Hydroxide Ions in Aqueous Systems. *Chem. Rev.* **2016**, *116* (13), 7642−7672.

(55) Sloutskin, E.; Tamam, L.; Sapir, Z.; Ocko, B. M.; Bain, C. D.; Kuzmenko, I.; Gog, T.; Deutsch, M. Counterions under a Surface-Adsorbed Cationic Surfactant Monolayer: Structure and Thermodynamics. *Langmuir* **2022**, *38* (40), 12356−12366.

(56) Li, P. X.; Dong, C. C.; Thomas, R. K.; Penfold, J.; Wang, Y. Neutron Reflectometry of Quaternary Gemini Surfactants as a Function of Alkyl Chain Length: Anomalies Arising from Ion Association and Premicellar Aggregation. *Langmuir* **2011**, *27* (6), 2575−2586.

(57) Phan, C. M.; Nguyen, C. V.; Nakahara, H.; Shibata, O.; Nguyen, T. V. Ionic Nature of a Gemini Surfactant at the Air/Water Interface. *Langmuir* **2016**, *32* (48), 12842−12847.

(58) Wegrzyńska, J.; Para, G.; Chlebicki, J.; Warszyński, P.; Wilk, K. A. Adsorption of Multiple Ammonium Salts at the Air/Solution Interface. *Langmuir* **2008**, *24* (7), 3171−3180.

(59) Casandra, A.; Tsay, R.-Y.; Phan, C.-M.; Lin, S.-Y. An Examination of the One-Parameter Adsorption Equation without Using the Gibbs Adsorption Equation. *Colloids Surf. A Physicochem. Eng. Asp.* **2017**, *512*, 137−144.

(60) Liang, X.; Michelsen, M. L.; Kontogeorgis, G. M. Pitfalls of Using the Geometric-Mean Combining Rule in the Density Gradient Theory. *Fluid Phase Equilib.* **2016**, *415*, 75−83.

(61) Li, P. X.; Li, Z. X.; Shen, H.-H.; Thomas, R. K.; Penfold, J.; Lu, J. R. Application of the Gibbs Equation to the Adsorption of Nonionic Surfactants and Polymers at the Air-Water Interface: Comparison with Surface Excesses Determined Directly Using Neutron Reflectivity. *Langmuir* **2013**, *29* (30), 9324−9334.

(62) Nguyen, K. T.; Nguyen, A. V.; Evans, G. M. Interfacial Water Structure at Surfactant Concentrations below and above the Critical Micelle Concentration as Revealed by Sum Frequency Generation Vibrational Spectroscopy. *J. Phys. Chem. C* **2015**, *119* (27), 15477−15481.

(63) Nakahara, H.; Shibata, O.; Rusdi, M.; Moroi, Y. Examination of Surface Adsorption of Soluble Surfactants by Surface Potential Measurement at the Air/Solution Interface. *J. Phys. Chem. C* **2008**, *112* (16), 6398−6403.

(64) Tanford, C. Thermodynamics of Micelle Formation: Prediction of Micelle Size and Size Distribution. *Proc. Natl. Acad. Sci. U.S.A.* **1974**, *71* (5), 1811−1815.

(65) Buckingham, S. A.; Garvey, C. J.; Warr, G. G. Effect of Head-Group Size on Micellization and Phase Behavior in Quaternary Ammonium Surfactant Systems. *J. Phys. Chem.* **1993**, *97* (39), 10236−10244.

(66) Engelhardt, K.; Peukert, W.; Braunschweig, B. Vibrational Sum-Frequency Generation at Protein Modified Air-Water Interfaces: Effects of Molecular Structure and Surface Charging. *Curr. Opin. Colloid Interface Sci.* **2014**, *19* (3), 207−215.